Vol. 68: 243–255, 2016
doi: 10.3354/cr01358

CLIMATE RESEARCH
Clim Res

Published May 4

Contribution to CR Special 32 'CLARIS-La Plata Basin: climate variability and uncertainties'

Contribution of cold fronts to seasonal rainfall in simulations over the southern La Plata Basin

Eduardo Marcos de Jesus[1], Rosmeri Porfírio da Rocha[1], Michelle Simões Reboita[2,*], Marta Llopart[3,4], Lívia Márcia Mosso Dutra[1], Armelle Reca C. Remedio[5]

[1]Department of Atmospheric Sciences, University of São Paulo, Rua do Matão, 1226 Cidade Universitária, São Paulo 05508-090, Brazil

[2]Natural Resources Institute, Federal University of Itajubá, Av. BPS 1303, Itajubá, Minas Gerais 37500-903, Brazil

[3]Departamento de Física, Universidade Estadual Paulista (UNESP), Bauru, São Paulo 17033-360, Brazil

[4]Centro de Meteorologia de Bauru (IPMet), Bauru, São Paulo, Brazil

[5]Climate Service Center Germany (GERICS) Chilehaus, Eingang B, Fischertwiete 1, Hamburg 20095, Germany

ABSTRACT: This work investigates how regional climate models REMO and RegCM4 simulate the frequency of cold fronts (CFs) over southern Brazil and the contribution of these systems to the seasonal precipitation over the southern part of La Plata Basin (SLPB) in South America. Simulations were driven by the ERA-Interim reanalysis and compared with local observations (from Rio Grande station; RG), ERA-Interim, and rainfall analysis from the Climate Prediction Center (CPC). CF identification was carried out objectively by considering (1) the turning of the meridional wind component from north to south and (2) a decrease in air temperature between 1 d before and 1 d after the CF passage. For the period 1991–2008, a mean of 55.3, 53.1 and 51.8 CFs yr^{-1} were identified, respectively, for RG (observed), REMO and RegCM4. These values show a small bias in the simulated annual frequency of CFs (around −5%), but the underestimation reaches −17% during summer in the RegCM4. In the simulations, it is possible to find some association between seasonal bias of rainfall and the bias of rainfall during CF periods (defined as extending from 2 d before to 2 d after the CF passage) over SLPB. Except in summer, RegCM4 presents stronger biases than REMO for rainfall for both CF periods and overall seasonal climatology. For the winter season, the CF composites indicate that deeper low pressure and larger availability of moisture at low levels (from 2 d before to the day of the CF) contribute to the small underestimation of rainfall in REMO (−5%) compared with RegCM4 (−25%).

KEY WORDS: Cold fronts · Precipitation · La Plata Basin · Regional climate models

1. INTRODUCTION

The weather and climate of southeastern South America (SA) are mostly controlled by cold fronts (CFs). These systems move from southwest to northeast over the continent and are responsible for phenomena such as strong winds, intense precipitation, localized cooling, frosts, and dispersion of pollutants out of the boundary layer. According to Satyamurty & Mattos (1989), Reboita et al. (2009) and Simmonds et al. (2012), the southern/southeastern coasts of SA are frontogenetic regions throughout the year. Cavalcanti & Kousky (2009) evaluated the seasonality of the CFs over SA using an objective methodology applied in the reanalysis from the National Centers for Environmental Prediction/National Center for Atmospheric Research (NCEP/NCAR; Kalnay et al. 1996) from 1979 to 2005. In this study, CFs are registered when, the following characteristics occur from the day before to the day of the CF: a decrease of ≥2°C in air temperature at 925 hPa; an increase of ≥2 hPa in sea level pressure; and turning of the

*Corresponding author: reboita@unifei.edu.br

meridional wind component from north to south, with a southerly wind component of ≥2 m s^{-1}. According Cavalcanti & Kousky (2009), the frequency of CFs over southeastern SA, which includes the La Plata Basin (LPB), is slightly higher during winter/spring, with an average of approximately 12 CFs, compared with summer with 10 CFs. Similar CF frequency for a period of 3 yr was obtained over the city of Rio Grande (~32° S, 52° W) located near the southern tip of Brazil (Britto & Krusche 1996).

Other studies focused on CF activity over specific regions of southern or southeastern Brazil can be mentioned. Silva et al. (2014) obtained an annual frequency of 27 CFs over southeastern Brazil (Minas Gerais state), with the highest number of CFs occurring during the winter and spring seasons. Over the coast of southern Brazil (Santa Catarina state), Rodrigues et al. (2004) found a weak seasonality of CFs, with slightly higher numbers during spring. Silva et al. (2014) and Rodrigues et al. (2004) have used similar methodology, i.e. meridional wind turning from north to south and temperature decreasing from 1 d before to 2 d after the CFs cross the region. The maximum of CFs in spring is similar to that obtained by Justi da Silva & Silva Dias (2002) and Andrade (2005), who in addition found a slight minimum in the frequency of CFs during summer and autumn. It is also important to mention that previous studies have highlighted the strong contribution of CFs to the seasonal rainfall over southeastern SA (e.g. Catto et al. 2012). For example, during the summer, the association of CFs with the South Atlantic Convergence Zone (SACZ) is well known, as shown by Oliveira (1986), Satyamurty et al. (1998), and Nieto-Ferreira & Chao (2011).

Studies evaluating the performance of climate models in simulating CF frequency over SA are not common. In this region, Andrade et al. (2012) compared the simulations from the Geophysical Fluid Dynamics Laboratory (GFDL) and Hadley Center global models with the NCEP/NCAR reanalysis. Both models overestimated the frequency of CFs.

Efforts have been organized to improve results of regional climate models (RCMs) over SA, such as the World Climate Research Project Coordinated Regional Downscaling Experiment (CORDEX; Giorgi et al. 2009) and A Europe–South America Network for Climate Change Assessment and Impact Studies in La Plata Basin (CLARIS-LPB; Solman et al. 2013). The goal of CLARIS-LPB was to evaluate regional climate change impacts and to develop adaptation strategies for the La Plata Basin (LPB). In this context, Solman et al. (2013) analyzed the performance in the present climate (1990–2008) of 7 RCMs (RCA, REMO, PROMES, RegCM3, MM5, LMDZ, and ETA) integrated with a horizontal grid spacing of about 50 km and driven by the ERA-Interim reanalysis (Dee et al. 2011). This study has shown a dry bias in the summer precipitation over LPB and from north to northwest SA. In winter, the dry bias was also present in LPB.

Solman et al. (2013) showed that over Uruguay, located in the southern LPB, only a few models are capable of capturing the peaks in the observed annual cycle of precipitation that occur in April and October. One of them is the REMO, which reproduces the observed precipitation amount in all months of the year while most models project very dry winter months compared with observation. The RegCM4 is one of the RCMs presenting large underestimation of precipitation over the southern LPB (Solman et al. 2013). This feature is a common shortcoming of many RCMs and global climate models (Reboita et al. 2014a, Vera & Silvestri 2009). In this context, since the different RCMs compared by Solman et al. (2013) have different parameterization schemes, we suggest that the dry biases could be due to some deficiencies in the simulation of mid-latitude systems as CFs that cross over the LPB. To evaluate this hypothesis, we analyzed the occurrence of CFs in the REMO and RegCM4 RCMs, since the former presents smaller errors in precipitation while the latter is part of the group of RCMs that have large dry biases over most of the LPB (Solman et al. 2013).

In summary, this work investigates how 2 RCMs used in the CLARIS-LPB project simulate the CFs over southern Brazil (which is part of the LPB region) and their contribution to the seasonal climatology of precipitation over the southern LPB (hereafter SLPB). Cold fronts simulated by the REMO (no dry bias) and RegCM4 (with dry bias) are compared with local observational and reanalysis data for the period 1991–2008.

2. DATA, MODELS AND METHODS

2.1. Data

For the period 1991–2008, local observations (sea level pressure, air temperature, and wind components) from the Rio Grande (RG) station were used to identify and characterize the CFs over SLPB. The RG station is a conventional meteorological station located at 32°04′ S, 52°10′ W (see Fig. 1), with a World Meteorological Organization (WMO) number

83995. This station was selected due to its location inside one of the most important frontogenetic (Satyamurty & Mattos 1989, Reboita et al. 2009) and cyclogenetic (Hoskins & Hodges 2005, Reboita et al. 2010) regions of the eastern coast of SA. In addition, the data from this station have been quality controlled in previous studies (Reboita et al. 2006).

Atmospheric variables from the ERA-Interim reanalysis (Dee et al. 2011), with horizontal grid spacing of 1.5 degrees, were used as initial and boundary conditions for the simulations and to validate the simulated environment associated with CFs. Daily precipitation from the Climate Prediction Center (CPC; Chen et al. 2008) analysis was employed to evaluate the simulated precipitation. CPC is a rain-gauge only analysis with a horizontal grid of 0.5 degrees.

2.2. RegCM4

The RegCM4 (Giorgi et al. 2012, Reboita et al. 2014b) is a hydrostatic model that solves the equations of a compressible atmosphere using finite differences. The vertical coordinate is sigma-pressure. RegCM4 has various physical parameterization schemes available. In the current study, one of the RegCM4 simulations carried out by Llopart et al. (2014) is analyzed. This simulation used the Biosphere Atmosphere Transfer Scheme (BATS; Dickinson et al. 1993) for representation of surface processes, the Community Climate Model version 3 (CCM3) parameterization for the radiative transfer in the atmosphere (Kiehl et al. 1996), the Holtslag et al. (1990) scheme to solve planetary boundary layer, and a mixed cumulus convection parameterization, which uses Grell (1993) over the continent and Emanuel (1991) over the ocean.

2.3. REMO

This study uses the regional climate model REMO (Jacob & Podzun, 1997, Jacob 2001, Jacob et al. 2001) version 2009 (Jacob et al. 2012, Solman et al. 2013). REMO is hydrostatic and solves the discretized primitive equations of atmospheric motion within a limited area. Having been developed previously at the Max Planck Institute for Meteorology and now continued at the Climate Service Center Germany (GERICS), REMO was used during CLARIS-LPB and included as part of the model evaluation framework of the CORDEX South America activities.

The physical core of REMO was based on the global circulation model ECHAM4 (Roeckner et al. 1996) and the dynamical core from the former weather prediction model of the German Weather Service (DWD; Majewski 1991). The large scale or stratiform cloud scheme of REMO is based on ECHAM4 and updated following ECHAM5, which included prognostic equations for cloud water, water vapor and cloud ice, and has empirical cloud cover scheme by Sundqvist et al. (1989). The convective (sub-grid) cloud parameterization in REMO is based on the mass-flux scheme from Tiedtke (1989) with the modifications of Nordeng (1994). The representation of the land surface utilizes a simple bucket soil water scheme (Dümenil & Todini 1992, Hagemann 2002, Rechid & Jacob 2006, Kotlarski 2007).

2.4. Simulations

The RegCM4 domain used 192 × 202 grid points in the north–south and west–east directions, with a horizontal grid spacing of about 50 km and 18 sigma-pressure levels in the vertical (da Rocha et al. 2012). The REMO domain coves 151 × 181 grid points in a rotated longitude-latitude coordinate system with a spatial resolution of 0.44° × 0.44° (about 50 km). The vertical levels in REMO are represented in a hybrid sigma-pressure coordinate system with 31 levels.

Both RegCM4 and REMO simulations followed the recommendation for the CORDEX South America domain (www.cordex.org). These simulations were nested in the ERA-Interim reanalysis (Dee et al. 2011). The RegCM4 simulation is for the period 1979–2009 and REMO was run from 1989 to 2008. However, only the period 1991–2008 is analyzed, since it corresponds to the period common to the simulations and the RG station dataset.

2.5. Methods

CFs were identified using the daily means of meridional wind at a height of 10 m and air temperature at 2 m. Following Rodrigues et al. (2004), the criteria for identification of CFs were (1) turning of the meridional wind component from the north to the south between the day before (day−1) and the day of the CFs (day0); and (2) a decrease of air temperature between day−1 and day0, and/or between day−1 and one day after (day+1) the identification of the CF. These criteria were applied to the observed and simulated data. Regarding the models, the atmospheric variables used to identify the CFs were selected considering the continental grid point nearest to the RG station. It is also important to mention that the use of daily averages of the atmospheric variables eliminates variations of scale smaller than diurnal, such as sea–land breezes (Rodrigues et al. 2004).

The analyses consisted of 3 parts: (1) description of the precipitation biases of RegCM4 and REMO over SLPB; (2) identification of the simulated and observed CFs and time evolution of the CFs' average characteristics from the prefrontal (day−2) to post-frontal (day+2) period; and (3) comparison of observed and simulated composite anomalies (sea level pressure, air temperature at 2 m height, and winds and specific humidity at 850 hPa) associated with the CFs. The southern part of LPB was defined as the area between 61°–48° W and 37°–27° S, excluding points over the sea, since the CPC analysis is available only over the continent (see box in Fig. 1).

3. RESULTS

3.1. Simulated precipitation in SLPB

The observed annual precipitation based on the CPC spatial pattern ranges from 2 to 5 mm d^{-1} over SLPB (not shown). The RegCM4 presents a strong negative precipitation bias (up to −2.5 mm d^{-1}) relative to the CPC over most of SLPB, mainly over southern Brazil and Uruguay (Fig. 1a), while a weaker overestimation of precipitation occurs in the REMO (Fig. 1b). The box shown in Fig. 1 corresponds approximately to the lower Parana River and Uruguay areas. In these regions, Solman et al. (2013) have indicated that most RCMs from the CLARIS-LPB Project underestimated rainfall, except REMO. A similar precipitation dry bias over the SLPB also occurs in most of CLARIS-LPB RCMs when they are forced by GCMs (Sanchéz et al. 2015).

Fig. 2 shows the annual cycle and the time series of the area-averaged precipitation over the SLPB. The observation from CPC characterizes the annual cycle of precipitation with 2 maxima of ~4.7 mm d^{-1} in April and October, and a minimum of ~2.2 mm d^{-1} in August (Fig. 2a). Overall, the phase and amplitude of the annual cycle of rainfall simulated by REMO are closer to the CPC observations than to those of RegCM4. REMO simulates the observed minimum and maximum precipitation in August and October, respectively; however, it is not able to capture the other observed rainfall peak in April. On other hand, RegCM4 simulates a different annual cycle of rainfall with only one maximum in February and a minimum in July, both of which are not observed in the CPC analysis. The Pearson correlation coefficients relative to CPC for the annual cycle of precipitation are 0.96 and 0.78 for REMO and RegCM4, respectively, which

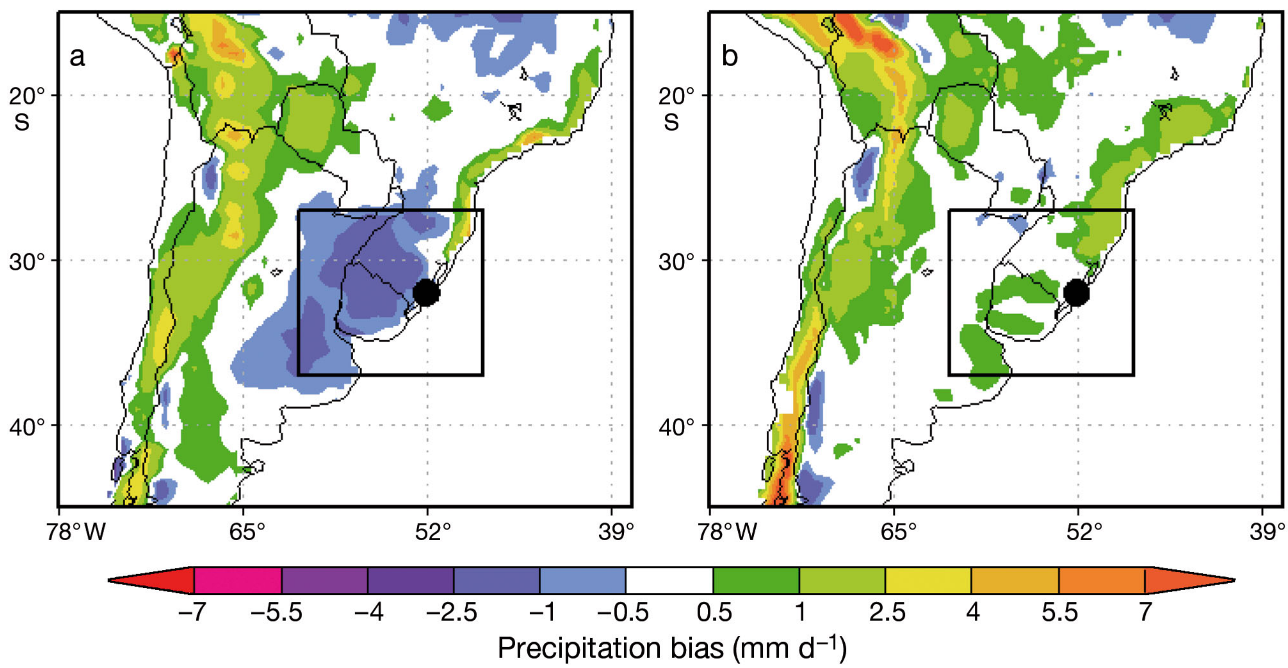

Fig. 1. Bias of annual precipitation of (a) RegCM4 and (b) REMO simulations from 1991 to 2008 in relation to Climate Prediction Center rainfall analysis. Box: southern La Plata Basin region; Black dot: Rio Grande station

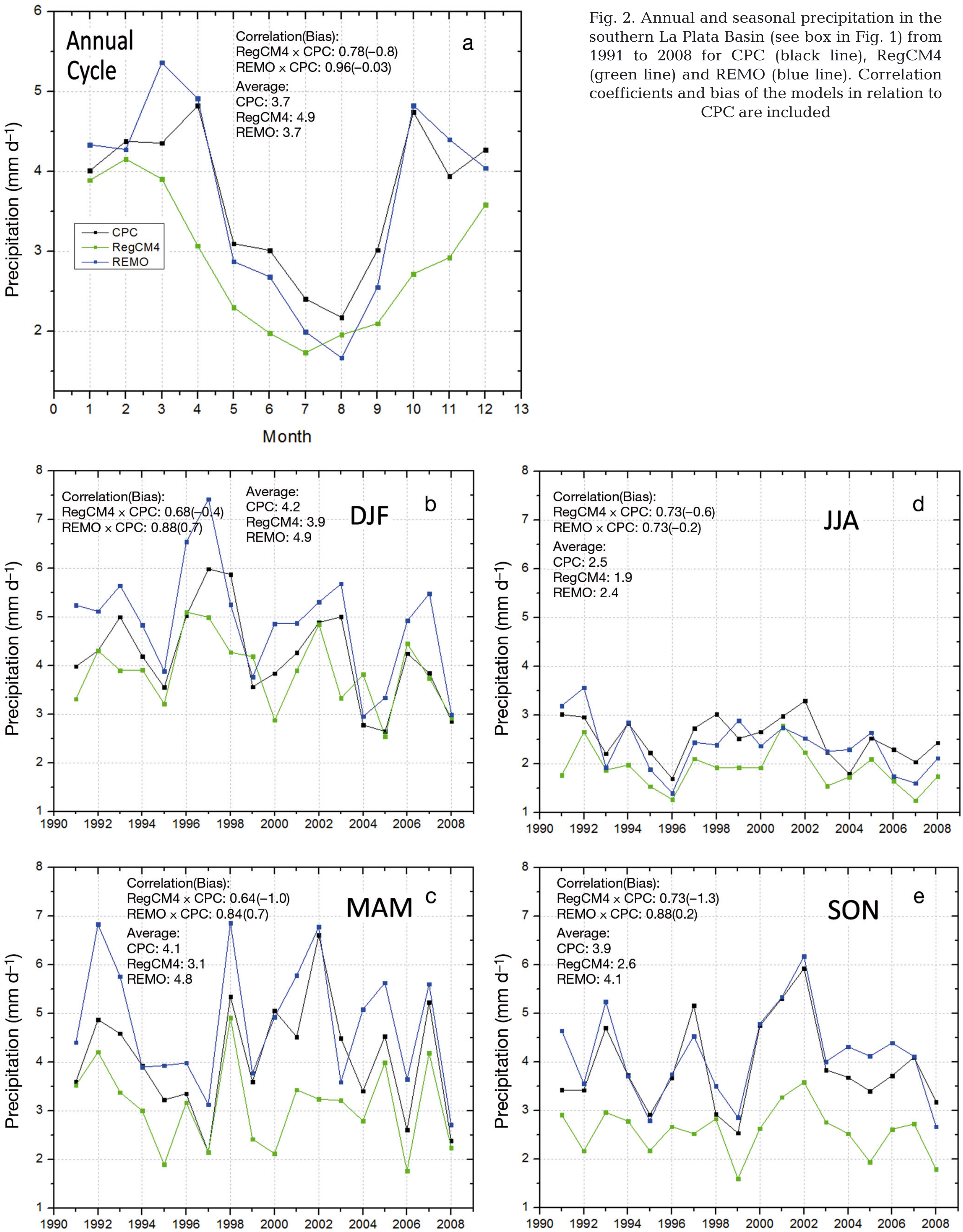

Fig. 2. Annual and seasonal precipitation in the southern La Plata Basin (see box in Fig. 1) from 1991 to 2008 for CPC (black line), RegCM4 (green line) and REMO (blue line). Correlation coefficients and bias of the models in relation to CPC are included

Table 1. Seasonal and annual average number of cold front passages observed at Rio Grande (RG) station and simulated in RegCM4 and REMO RCMs for the 1991–2008 period. Parentheses: relative biases (%) of the simulations in relation to the observational dataset, calculated from [(number simulated − number observed)/number observed] × 100%

	DJF	MAM	JJA	SON	Annual
RG observation	13.7	13.3	14.1	14.2	55.3
RegCM4	11.4	12.7	13.7	14.0	51.8
Relative bias (%)	(−17)	(−5)	(−3)	(−1)	(−6)
REMO	13.2	13.3	13.2	13.4	53.1
Relative bias (%)	(−4)	(0)	(−6)	(−6)	(−4)

indicates a better agreement between REMO and the CPC analysis. Moreover, REMO has a smaller bias for annual precipitation (−0.03 mm d^{-1}) than RegCM4 (−0.83 mm d^{-1}).

Regarding the inter-annual variability of precipitation for each season (Fig. 2b–e), the correlation coefficient between REMO and the CPC observations is higher (with a maximum of 0.88 in spring–summer) than between RegCM4 and the CPC. The higher correlation indicates a large agreement of REMO in the reproduction of the observed inter-annual precipitation variability. In most of the seasons, the precipitation biases are smaller in REMO than in RegCM4. The smaller biases in REMO occur in winter (−0.15 mm d^{-1}) and spring (+0.23 mm d^{-1}). RegCM4 has smaller seasonal bias (−0.35 mm d^{-1}) than REMO (+0.68 mm d^{-1}) only during summer. Similar results have been found by Solman et al. (2013), who by comparing 7 RCMs concluded that REMO better simulates the annual cycle and the amount of rainfall over most of the LPB.

3.2. Frequency of cold front occurrences

For the period 1991–2008, Table 1 presents the observed and simulated frequency of CFs and the RCMs' relative biases. The frequency of CFs at the RG station presents weak seasonality, i.e. from 14.2 in spring to 13.3 in autumn (Table 1). This value agrees with Britto & Krusche (1996) who evaluated CFs at the same station and with other CF studies over southeastern SA (Rodrigues et al. 2004, Cavalcanti & Kousky 2009, Andrade et al. 2012). The weak seasonality of CFs at RG also agrees with that of the cold surges associated with systems crossing SA (Garreaud 1999), with the climatology of Southern Hemisphere mobile fronts (Simmonds et al. 2012) and with the CFs identified over southern Brazil (Rodrigues et al. 2004, Cavalcanti & Kousky 2009). These comparisons support the methodology used in the present study for identifying the CFs.

The REMO simulates the weak seasonality of CF frequency present in the observations, with about 13.3 systems per season and has an annual relative bias of only 4.0% (Table 1). Considering each season, REMO's underestimation of the number of CFs is small, with a maximum of −6% in winter and spring. RegCM4 simulates a low frequency of CFs in summer (11.4) and a high frequency in spring (14.0), providing a seasonal range of 2.6 systems. This range is greater than the observed value of 0.9, and indicates higher seasonality compared with the RG station. The negative bias for the total number of CFs in RegCM4 (−6%) is mainly due to the large underestimation of CFs in summer (−17%). In other seasons, the relative bias of RegCM4 CFs is <−5%.

The time evolution of the mean environmental conditions from 2 days before (day−2) until 2 days after (day+2) the CFs' passage (day 0) is presented in Fig. 3. For all seasons and in agreement with the RG observations, the RegCM4 and REMO capture the time evolution of the meridional wind component, which turns from north to south (from negative to positive values) between the day before (day−1) and the day of the CF (day0). Generally, the simulated meridional wind speeds are similar to the observed values, except on day−2 when they are greater than those observed at RG. During the CF passages, simulations also capture the time evolution of the air temperature and sea level pressure observed at RG, but the biases depend on the season. RegCM4 is colder than the RG observations during the austral autumn and winter, while the biases are small in summer and spring (Fig. 3). In all seasons, the air temperature simulated by REMO is closer to observations than those simulated by RegCM4, except on day+2 when REMO is systematically colder than RG, indicating colder postfrontal air in REMO than observed at RG (see section 3.3.). For sea level pressure, RegCM4 has a systematic negative bias compared to the observations, which is large during austral summer–spring (Fig. 3). REMO has a small positive bias for sea level pressure from day−2 until day+2, except during austral winter.

The comparisons of precipitation associated with a CF episode requires caution since it has a high spatial variability. For this analysis, RCM outputs were interpolated to the CPC horizontal grid (with 0.5° of grid spacing) and only one grid point is used to represent the RG station. Even with these constraints, simulations are able to reproduce the time evolution

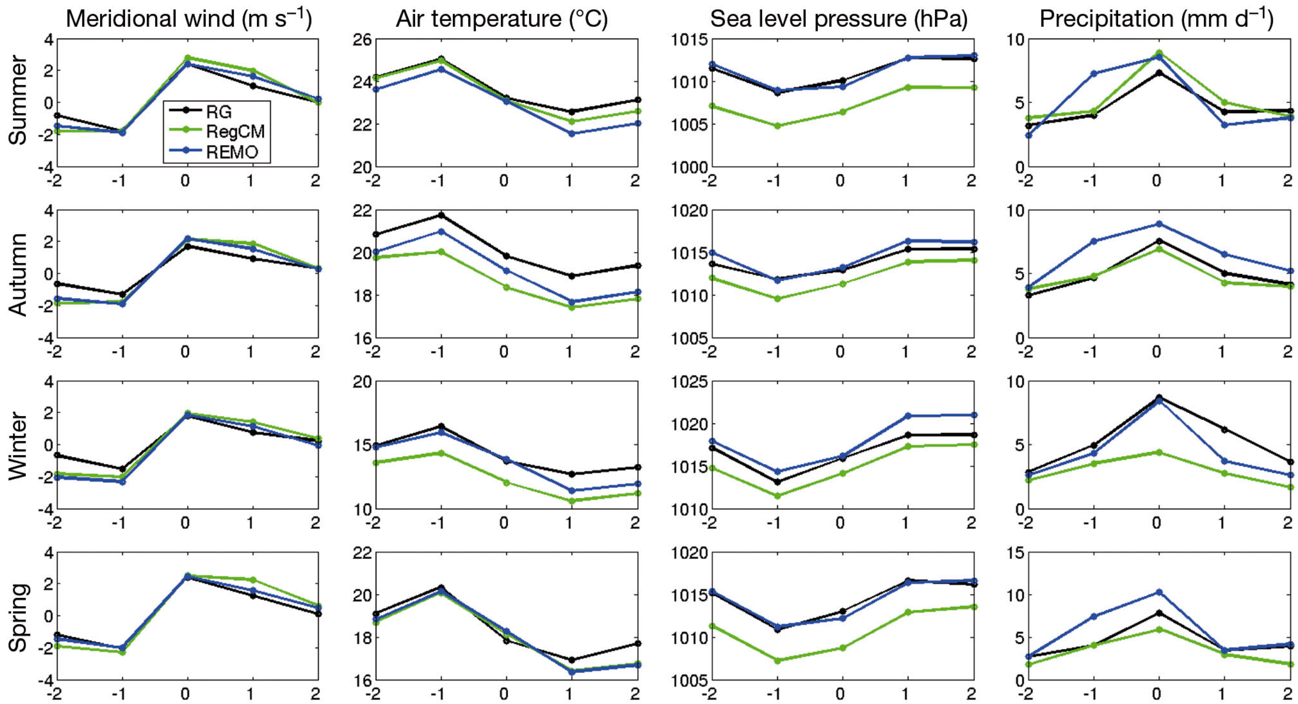

Fig. 3. Seasonal temporal evolution (from day−2 to day+2) of average environmental conditions during cold fronts: meridional wind (m s^{-1}, first column), air temperature (°C, second column), sea level pressure (hPa, third column) and precipitation (mm d^{-1}, 4th column) as obtained from Rio Grande station (RG; black line), RegCM4 (green line) and REMO (blue line). For precipitation, CPC grid point values were used instead of local measurements at RG

of observed rainfall, with the maximum rainfall rate occurring on day0 (Fig. 3). RegCM4 overestimates the precipitation from day−2 to day+1 during summer and underestimates it from day−1 to day+1 in the other seasons. During autumn, REMO overestimates the precipitation from day−2 to day+2. For the other seasons REMO simulates larger amounts of precipitation for day−1, i.e. it tends to have higher prefrontal rainfall rate than that observed by CPC.

For the period 1991–2008 (18 yrs), Table 2 shows the relative biases for precipitation in the SLPB region (box in Fig. 1) for the seasonal average (climatology) and only the accumulated rainfall during the CF period (from day−2 until day+2, i.e. during 5 d). It is worth mentioning that CFs make a large contribution to the seasonal rainfall, from 84 % during autumn to 91 % in spring in CPC. In RegCM4 the seasonal underestimation of rainfall associated with CF periods is large (from −25 to −36 %), which contributes to the large climatological dry bias, except in summer. For example, on an annual scale RegCM4 presents a dry bias of −30 % during the CFs and −22 % for the climatology. These biases emphasize the contribution of the CFs to the climatological dry bias in RegCM4. In REMO, the relative rainfall biases during the CF periods and climatology have similar magnitudes, indicating a large contribution of REMO-simulated CFs to the seasonal precipitation bias (Table 2). For REMO, the climatological and CF biases are positive during summer–autumn and spring and negative in winter. However, in most of the seasons the relative rainfall underestimations (climatological and for CF periods) are smaller in REMO than RegCM4, except for the climatological bias in summer.

Table 2. Relative biases (%) of precipitation for model climatology and for the 5 d (from day−2 until day+2) centered around the cold front (CF) passages in the southern La Plata Basin (SLPB) region (see Fig. 1), for the period 1991–2008 (18 yr). Relative bias is calculated as in Table 1 [([model−observation]/observation) × 100 %]. We computed it to the precipitation climatology (for the whole period of study) and to the precipitation associated only with CFs (from day−1 to day+1)

	DJF	MAM	JJA	SON	Annual
RegCM4					
Climatic bias (%)	−8.0	−24.0	−25.0	−34.0	−22.0
CFs bias (%)	−25.0	−31.0	−30.0	−36.0	−30.0
REMO					
Climatic bias (%)	16.0	17.0	−5.0	6.0	10.0
CFs bias (%)	16.0	22.0	−8.0	5.0	11.0

3.3. Cold front composites

The calculation of composite fields for the CFs contributes to the understanding of the mean synoptic environment during the CF events and also to the discussion of the simulated seasonal bias of rainfall. For brevity, only the anomalies are shown, i.e. the difference between the composites for the dates with CFs and the seasonal climatology. Since the composites in each season have similar spatial pattern, only that for the winter is presented because underestimation of rainfall is strong in RegCM4 (−25%) and small in REMO (−5%).

For the winter season, Fig. 4 shows the prefrontal (day−1) to postfrontal (day+1) anomalies of the sea level pressure and 2 m air temperature. The cold and warm fronts are not drawn in Fig. 4, but by the stretching of the isobars, it is possible to infer the places of these systems. For day−1, ERA-Interim locates the boundary between warm and cold anom-

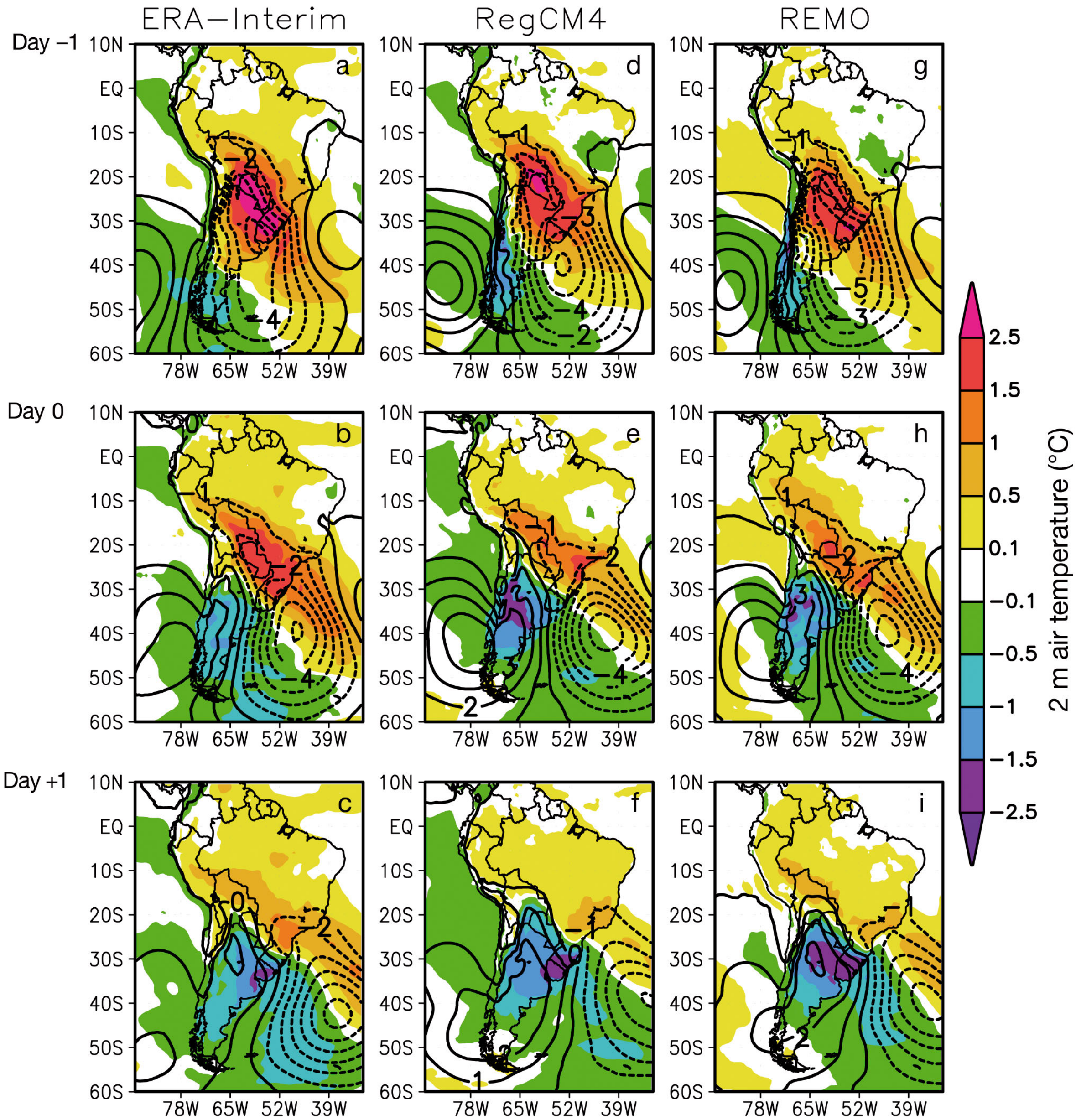

Fig. 4. Winter composite maps of sea level pressure (hPa, black contours) and 2 m air temperature (colours) anomalies for day−1 (top), day0 (middle) and day+1 (bottom) from cold front passages from the ERA-Interim reanalysis (left), RegCM4 (middle), and REMO (right). For sea level pressure, the solid (dashed) lines indicate positive (negative) anomalies. Anomalies are calculated as departures from seasonal mean

alies of air temperature over central Argentina and shows a large area of warm air over Paraguay and extreme southern Brazil (Fig. 4a). The postfrontal cold air covers the southern parts of Argentina and Chile. This spatial pattern is similar to that obtained by Cavalcanti & Kousky (2009) for CFs identified over a grid point inside LPB (30° S, 52.5° W). During the prefrontal day, the anomalous low-pressure center (−5 hPa) is located over northeastern Argentina and Uruguay, and the cold front (CF) extends from northeastern Argentina to Bolivia. Both RegCM4 and REMO simulate the cold air over southern Argentina–Chile but displaced northward compared with ERA-Interim (Figs. 4d–g). The postfrontal anticyclone is also displaced northward and is more intense in the simulations than in ERA-Interim (Figs. 4a,d,g). However, REMO simulated the location of the anomalous low-pressure center closer to the ERA-Interim than did RegCM4. In the latter, the anomalous low-pressure center is displaced southeastward compared to ERA-Interim (Figs. 4a–d). In both models the pressure anomaly in the center of the cyclone is −6 hPa.

For day0, ERA-Interim locates the anomalous low pressure center over the South Atlantic Ocean (40° S, 48° W), with the CF extending to Bolivia and crossing the RG station (Fig. 4b). Again, this observed pattern agrees with the Cavalcanti & Kousky (2009) analysis of CFs. In the RCMs (Figs. 4e–h), the anomalous low-pressure area is displaced eastward compared with ERA-Interim. In addition, the negative anomalies of pressure over southern Brazil are weaker in RegCM4 (2–3 hPa) than in REMO (3–4 hPa), with REMO values closer to the ERA-Interim. The boundary between the anomalous cold and warm air is now over Uruguay–northeastern Argentina in the reanalysis but it is shifted northward in the simulations. The simulations and ERA-Interim show the postfrontal cold area covering most of Argentina and Chile, while the prefrontal warm air is in south-southeastern Brazil and Paraguay. However, the warm sector is more pronounced in ERA-Interim than in the simulations, while the opposite occurs in relation to the cold sector. Although some differences were observed in the location and intensity of cold and warm areas between ERA-Interim and simulations on day0, there is a similarity of position of the CF in the simulations and ERA-Interim.

During day+1, in the ERA-Interim (Fig. 4c) the postfrontal anomalous anticyclone reaches RG and the CF is over southeastern Brazil. The simulated CF position is similar to that of ERA-Interim, but the postfrontal anticyclone and associated cold air, and the low-pressure system are displaced eastward compared to the reanalysis (Figs. 4f–i). As in day0, in day+1 the anomaly in the cold air is stronger than that in the warm air in the simulations.

Fig. 5 presents the CFs′ anomalies for specific humidity and wind at 850 hPa. At day−1, there is a low level jet in ERA-Interim, extending from northern Bolivia, through Paraguay, Uruguay and extreme southern Brazil (Fig. 5a). This same area exhibits confluence and larger amount of moisture in the atmosphere. Drier postfrontal air covers the Southern Pacific Ocean and the southern tip of SA. In the simulations, the drier postfrontal air is displaced northward compared to ERA-Interim (Figs. 5d–g). The REMO simulates prefrontal positive values of specific humidity anomalies closer to ERA-Interim than does the RegCM4. The higher moisture environment at low levels (which may result from large moisture flux convergence) in the REMO over extreme southern Brazil-Uruguay may explain its higher positive precipitation anomaly over SLPB on day−1 shown in Fig. 6. Moreover, the area coverage of positive anomalies of precipitation in the REMO (Fig. 6g) is more similar to CPC (Fig. 6a) than is the RegCM4 (Fig. 6d).

For day0, the simulated anomalous cyclonic circulation at 850 hPa is displaced eastward compared to the ERA-Interim, as is also noted for the low pressure at the surface (Figs. 5b,e,h). In ERA-Interim, the positive anomaly of specific humidity concentrates in a narrow northwest–southeast band, and is limited to the south by drier air covering central-southern Argentina (Fig. 5b). REMO (Fig. 5h) overestimates the intensity of postfrontal dry air over Uruguay and eastern Argentina compared to ERA-Interim and RegCM4. In the warm sector over Paraguay and Bolivia, REMO presents more moisture than RegCM4 (Figs. 5e–h). REMO also simulates a deeper anomalous low-pressure area than RegCM4 over southern Brazil (Figs. 4e–h). Both features may explain the higher intensity of positive precipitation anomalies over SLPB in REMO, which is similar to CPC (Figs. 6b–h).

One day after the CFs cross RG (day+1), there is negative specific humidity anomaly over this area in ERA-Interim and models. In addition, 850 hPa atmospheric patterns (cyclonic and anticyclonic circulations) in the simulations are slightly displaced eastward compared to the ERA-Interim.

From day−1 to day0, RegCM4 simulates a weaker positive anomaly of rainfall covering a larger area than in CPC (Fig. 6). In REMO the area of the positive anomaly of rainfall is closer to CPC, but the intensity is higher. For day+1 the positive anomaly of rainfall associated with the CFs covers southern Brazil and Paraguay in the CPC analysis, while it is slightly shifted northward in the simulations (Figs. 6c,f,i).

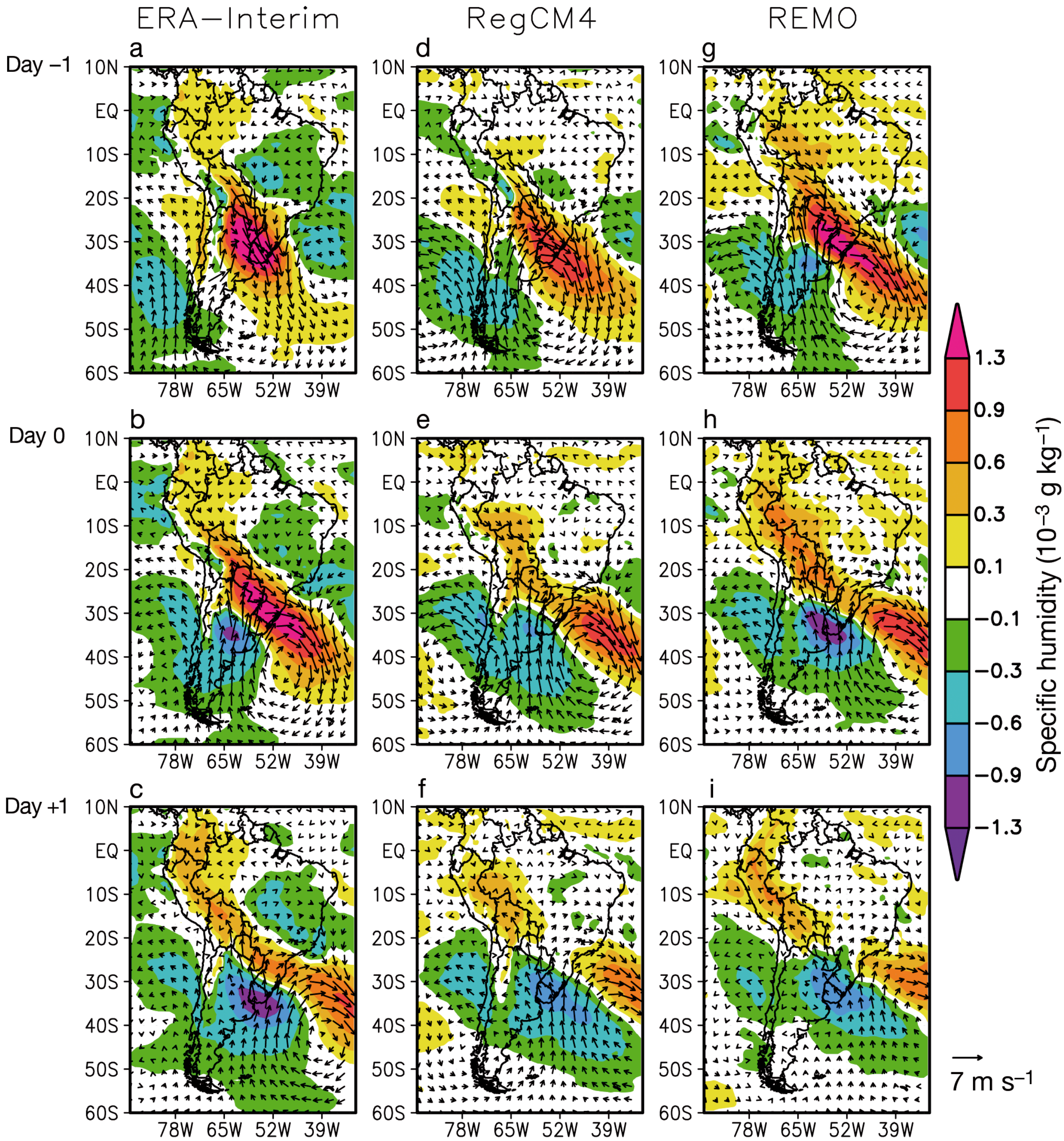

Fig. 5. Winter composite maps of wind vectors (arrows) and specific humidity (color) at 850 hPa, anomalies for day−1 (top), day0 (middle) and day+1 (bottom) from cold front passages from ERA-Interim reanalysis (left), RegCM4 (middle), and REMO (right). Anomalies are calculated as departures from seasonal mean

4. CONCLUSIONS

An analysis of 2 regional climate models (REMO and RegCM4) used in the CLARIS-LPB project is presented. For the period 1991–2008, the simulated climatology of cold fronts (CFs) over southern Brazil and its contribution to the precipitation in the southern part of La Plata Basin (SLPB) were investigated. An objective methodology, which considers the wind shift and negative trends of air temperature, was applied to identify CFs in the observation and simulations.

For the period 1981–2008, RegCM4 presents a large negative bias (−22 %) for annual rainfall rate, while the bias is positive and small (10 %) in REMO over SLPB. Considering each season, RegCM4 negative rainfall bias varies from −8 % in summer to −34 % in spring. In REMO the rainfall bias ranges from −5 % in winter up to 17 % in autumn. In most seasons of the year, REMO simulates smaller rainfall biases than

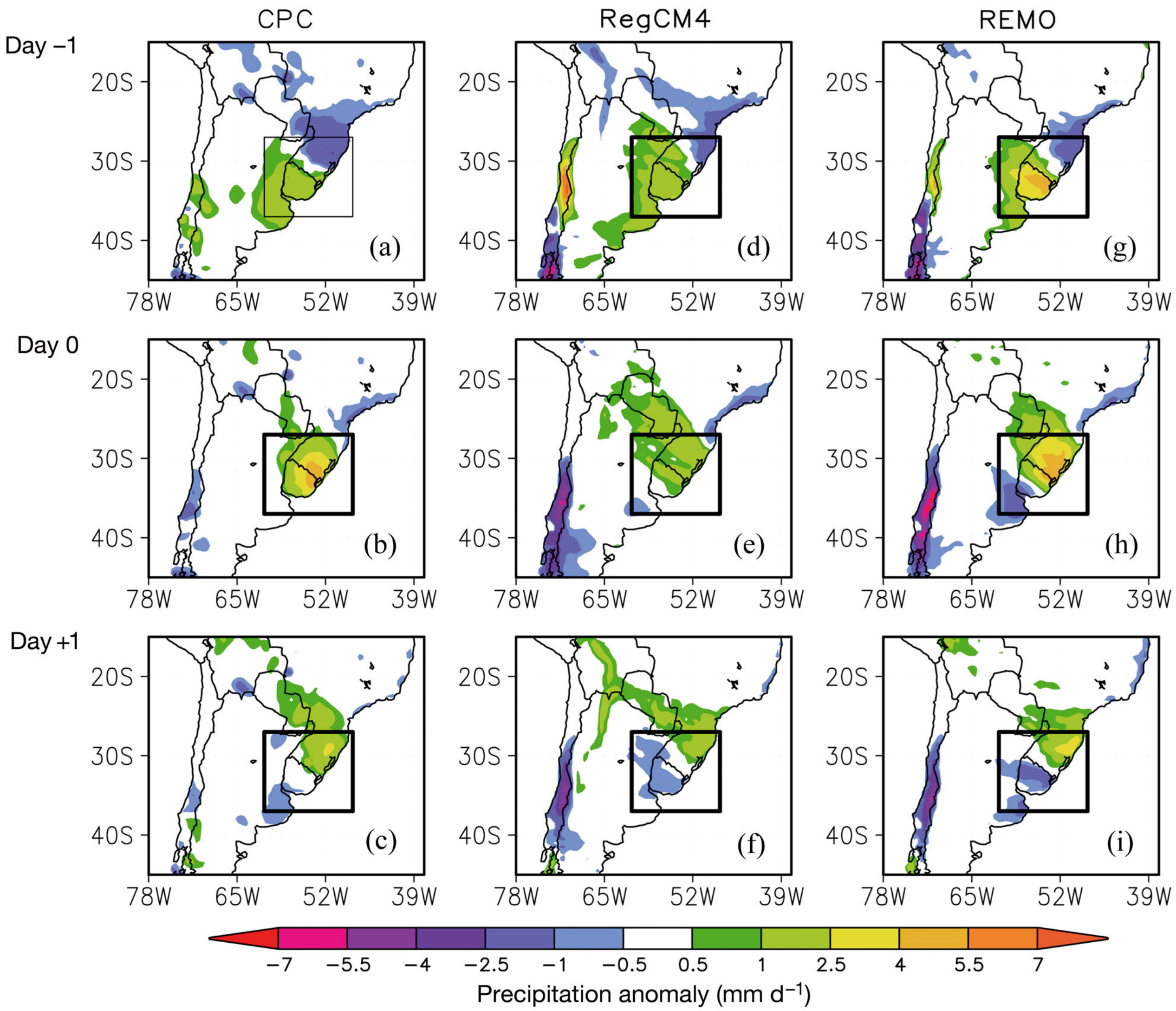

Fig. 6. Winter composite maps of precipitation anomaly for day−1 (top), day0 (middle) and day+1 (bottom) from cold front passages from Climate Prediction Center (CPC) analysis (left), RegCM4 (middle), and REMO (right). Box: southern La Plata Basin location defined in the present study. Anomalies are calculated as departures from seasonal mean

RegCM4. An important feature is the small bias of precipitation in REMO during winter (–5%) and spring (+6%) over the SLPB.

A mean of 55.3, 53.1 and 51.8 CFs yr^{-1} were identified crossing southern Brazil at RG (observed), for REMO and for RegCM4, respectively. Thus, the simulations have a small bias (around −5%) for the CF climatology, but the underestimate reaches −17% during summer in RegCM4. The number of CFs identified at RG ranged from 14.2 (spring) to 13.3 (autumn) indicating the weak seasonality of CFs. This feature is better simulated by REMO than by RegCM4. Simulations are able to reproduce the observed seasonal time evolution of atmospheric variables (wind, air temperature, sea level pressure and precipitation) from 2 d before until 2 d after the CFs over southern Brazil.

For the RG station, >84% of the precipitation shown by CPC in every season occurs during periods with cold frontal passages (from day−2 to day+2 of the CF), i.e. CFs are the main mechanism for seasonal rainfall. The underestimation of the precipitation in CF periods by RegCM4 varies from −25% in summer to −36% in spring. In absolute value, the relative errors in CF rainfall are smaller in REMO than in RegCM4. On an annual scale, RegCM4 presents major underestimation of rainfall (−30%) during CF periods reflected in the large negative bias of rainfall in its climatology (−22%). In REMO these errors are smaller and of similar magnitude (11% for CF periods and 10% for climatology). Therefore, both simulations indicate some association between their climatological precipitation biases and those during CF periods.

For winter CF periods, the REMO composites (from day−1 to day+1 of the CF passage) indicate a more favorable environment for precipitation, that is, large availability of moisture at low levels and deeper anomalous low pressure. Both features may explain the larger rainfall rate in REMO and it small underestimation of rainfall (−5%) compared to RegCM4 (−25%).

The present analysis considered only 2 of the 7 RCMs used in the CLARIS-LPB project (Solman et al. 2013). In future work it would be interesting to include a larger number of these RCMs to make a similar analysis. This will permit better understanding of the contribution of cold frontal periods to the underestimation of rainfall in these RCMs over most of LPB.

Acknowledgements. The authors thank CNPq (155700/2010-3, 307202/2011-9, 249244/2013-6, 474929/2012-2) and CAPES for financial support and CLARIS LPB (A Europe-South America Network for Climate Change Assessment and Impact Studies in La Plata Basin) EU-FP7 project (proposal 212492) and ICTP for providing the data.

LITERATURE CITED

Andrade KM (2005) Climatologia e comportamento dos sistemas frontais sobre a América do Sul. MSc. thesis, National Institute of Space Science, São José dos Campos

Andrade KM, Muller G, Cavalcanti IFA, Long MEF, Bidegain M, Berri G (2012) Avaliacão de mudancas na frequência de sistemas frontais sobre o sul da América do Sul em projecões do clima futuro. Meteorológica 37: 15–26

Britto FP, Krusche N (1996) Frequência e intensidade das frentes frias em Rio Grande. IX Congresso Brasileiro de Meteorologia. Campos do Jordão, São Paulo, p 185–188

Catto JL, Jakob C, Berry G, Nicholls N (2012) Relating global precipitation to atmospheric fronts. J Geophys Res Atmos 39:L10805, doi:10.1029/2012GL051736

Cavalcanti IFA, Kousky VE (2009) Frentes frias sobre o Brasil. In: Cavalcanti IFA, Ferreia NJ, Justi da Silva MGA, Silva Dias MAF (eds) Tempo e Clima no Brasil. Oficina Textos, São Paulo, p 135–147

Chen M, Shi W, Xie P, Silva V, Kousky V, Higgins RW, Janowiak K (2008) Assessing objective techniques for gauge-based analyses of global daily precipitation. J Geophys Res 113:D04110, doi:10.1029/2007JD009132

da Rocha RP, Cuadra SV, Reboita MS, Kruger LF, Ambrizzi T, Krusche N (2012) Effects of RegCM3 parameterizations on simulated rainy season over South America. Clim Res 52:253–265

Dee DP, Uppala SM, Simmons AJ, Berrisford P and others (2011) The ERA-Interim reanalysis: configuration and performance of the data assimilation system. QJR Meteorol Soc 137:553–597

Dickinson RE, Henderson-Sellers A, Kennedy PJ (1993) Biosphere−Atmosphere Transfer Scheme (BATS) version 1E as coupled to the NCAR community climate model. Tech Note NCAR/TN-3871STR, NCAR, Boulder, CO

Dümenil L, Todini E (1992) A rainfall-runoff scheme for use in the Hamburg climate model. In: O'Kane JP (ed) Advances in theoretical hydrology: a tribute to James Dooge. Eur Geophys Soc Ser Hydrol Sci 1, Elsevier Press Amsterdam, p 129–157

Emanuel KA (1991) A scheme for representing cumulus convection in large-scale models. J Atmos Sci 48:2313–2335

Garreaud RD (1999) Cold air incursions over subtropical and tropical South America. A numerical case study. Mon Weather Rev 127:2823–2853

Giorgi F, Coppola E, Solmon F, Mariotti L and others (2012) RegCM4: model description and preliminary tests over multiple CORDEX domains. Clim Res 52:7–29

Giorgi F, Jones C, Asrar G (2009) Addressing climate information needs at the regional level: the CORDEX framework. WMO Bull 58:175–183

Grell GA (1993) Prognostic evaluation of assumptions used by cumulus parameterizations. Mon Weather Rev 121: 764–787

Hagemann S (2002) An improved land surface parameter dataset for global and regional climate models. MPI-M, Rep 336, Hamburg

Holtslag A, de Bruijn E, Pan HL (1990) A high resolution air mass transformation model for short-range weather forecasting. Mon Weather Rev 118:1561–1575

Hoskins BJ, Hodges KI (2005) A new perspective on Southern Hemisphere storm tracks. J Clim 18:4108–4129

Jacob D (2001) A note to the simulation of the annual and inter-annual variability of the water budget over the Baltic Sea drainage basin. Meteorol Atmos Phys 77: 61–73

Jacob D, Van den Hurk BJJM, Andræ U, Elgered G and others (2001) A comprehensive model intercomparison study investigating the water budget during the BALTEX-PIDCAP period. Meteorol Atmos Phys 77:19–43

Jacob D, Elizalde A, Haensler A. Hagemann S and others (2012) Assessing the transferability of the regional climate model REMO to Different COordinated Regional Climate Downscaling EXperiment (CORDEX) regions. Atmosphere (Toronto) 3:181–199

Jacob D, Podzun R (1997) Sensitivity studies with the Regional Climate Model REMO. Meteorol Atmos Phys 63:119–129

Justi da Silva MGA, Silva Dias MAF (2002) A freqüência de fenômenos meteorológicos na América do Sul: uma climatologia. In: XII Congresso Brasileiro de Meteorologia, 2002, Sociadade Brasileira de Meteorologia, Foz do Iguacu

Kalnay E, Kanamitsu M, Kistler R, Collins W and others (1996) The NCEP/NCAR 40-year reanalysis project. Bull Am Meteorol Soc 77:437–470

Kiehl J, Hack J, Bonan G, Boville B, Breigleb B, Williamson D, Rasch P (1996) Description of the NCAR community climate model (CCM3). NCAR Tech Note NCAR/TN-420 + STR. NCAR, Boulder, CO

Kotlarski S (2007) A subgrid glacier parameterisation for use in regional climate modelling. PhD thesis, University at Hamburg

Llopart M, Coppola E, Giorgi F, da Rocha RP, Cuadra SV

(2014) Climate change impact on precipitation for the Amazon and La Plata basins. Clim Change 125:111–125

Majewski D (1991) The Europa-Modell of the Deutscher Wetterdienst. ECMWF seminar on numerical methods in atmospheric models 2:147–191

Nieto-Ferreira R, Chao WC (2011) Aqua-planet simulations of the formation of the South Atlantic Convergence Zone. Int J Climatol 33:615–628

Nordeng TE (1994) Extended versions of the convective parametrization scheme at ECMWF and their impact on the mean and transient activity of the model in the tropics. ECMWF Research Department, Tech Memo 206, ECMRWF, Reading

Oliveira AS (1986) Interacões entre sistemas frontais na América do Sul e a conveccão da Amazônia. MSc. thesis, INPE, São José dos Campos

Reboita MS, Krusche N, Piccoli HC (2006) Climate variability in Rio Grande, RS, Brazil: a quantitative analysis of contributions due to atmospheric systems. Rev Bras Meteorol 21:256–270

Reboita MS, Ambrizzi T, da Rocha RP (2009) Relationship between the Southern Annular Mode and Southern Hemisphere Atmospheric Systems. Rev Bras Meteorol 24:48–55

Reboita MS, da Rocha RP, Ambrizzi T, Sugahara S (2010) South Atlantic Ocean cyclogenesis climatology simulated by regional climate model (RegCM3). Clim Dyn 35: 1331–1347

Reboita MS, da Rocha RP, Dias CG, Ynoue RY (2014a) Climate projections for South America: RegCM3 driven by HadCM3 and ECHAM5. Adv Met doi:10.1155/2014/376738

Reboita MS, Fernandez JPR, Llopart MP, da Rocha RP, Pampuch LA, Cruz FT (2014b) Assessment of RegCM4.3 over the CORDEX South America domain: sensitivity analysis for physical parameterization schemes. Clim Res 60: 215–234

Rechid D, Jacob D (2006) Influence of monthly varying vegetation on the simulated climate in Europe. Meteorol Z 15:99–116

Rodrigues GLM, Franco D, Sugahara S (2004) Climatologia de Frentes Frias no litoral de Santa Catarina. Revista Brasileira de Geofísica 22:135–151

Roeckner E and others (1996) The atmospheric general circulation model ECHAM-4: model description and simulation of present day climate. MPI-M Rep 218

Sánchez E, Solman S, Remedio ARC, Berbery H and others (2015) Regional climate modelling in CLARIS-LPB: a concerted approach towards twentyfirst century projections of regional temperature and precipitation over South America. Clim Dyn 45:2193–2212

Satyamurty P, Mattos LF (1989) Climatological lower tropospheric frontogenesis in the midlatitudes due to horizontal deformation and divergence. Mon Weather Rev 117: 1355–1364

Satyamurty P, Nobre CA, Silva Dias PL (1998) South America. In: Karoly DJ, Vicent DG (eds) Meteorology of the Southern Hemisphere 27:119–139

Silva LJ, Reboita MS, da Rocha RP (2014) Relacão da passagem de frentes frias na região sul de Minas Gerais (RSMG) com a precipitacão e eventos de geada. Rev Bras Clim 14:229–246

Simmonds I, Keay K, Bye JAT (2012) Identification and climatology of Southern Hemisphere mobile fronts in a modern reanalysis. J Clim 25:1945–1962

Solman S, Sanchez E, Samuelsson P, da Rocha RP and others (2013) Evaluation of an ensemble of regional climate model simulations over South America driven by the ERA-Interim reanalysis: model performance and uncertainties. Clim Dyn 41:1139–1157

Sundqvist H, Berge E, Kristjansson JE (1989) Condensation and cloud parameterization studies with a mesoescale numerical weather precipitation model. Mon Weather Rev 117:1641–1657

Tiedtke M (1989) A comprehensive mass flux scheme for cumulus parameterization in large scale models. Mon Weather Rev 117:1779–1800

Vera C, Sivestri G (2009) Precipitation interannual variability in South America from the WCRP-CMIP3 multi-model dataset. Clim Dyn 32:1003–1014

Editorial responsibility: Enrique Sanchez (Guest Editor), Toledo, Spain

Submitted: August 17, 2015; Accepted: November 22, 2015
Proofs received from author(s): February 17, 2016